Comparison of Mobile-Radar Measurements of Tornado Intensity with Corresponding WSR-88D Measurements

M. TOTH AND R. J. TRAPP

Department of Earth, Atmospheric, and Planetary Sciences, Purdue University, West Lafayette, Indiana

J. WURMAN AND K. A. KOSIBA

Center for Severe Weather Research, Boulder, Colorado

(Manuscript received 7 March 2012, in final form 3 October 2012)

ABSTRACT

In the United States, visual observations of tornadoes and/or the existence of tornado damage currently provide the sole evidence of tornadogenesis in association with a mesocyclone or other radar-detected storm-scale vortex. The severity of the tornado damage is currently the only means of estimating the intensity of tornadoes, radar detected or otherwise. The limitations of the damage-based record of tornado occurrence and intensity are well known and motivated this research. Weather Surveillance Radar-1988 Doppler (WSR-88D) measurements of the translating tornadic flow were compared with (semi-) coordinated measurements obtained near the surface with mobile radar. On the basis of a small yet fairly broad sample of tornadoes, high linear correlation was found between the vortex intensity (rotation plus translation) quantified using WSR-88D data and that quantified using Doppler on Wheels data. The possible effects of Doppler radar sampling on these results were explored through experiments with a simple vortex model. These experiments argued that the likelihood is high that a tornado would be sampled in a favorable way during at least one radar scan. Hence, the suggestion from this work is that WSR-88Ds (or similar operational radars) can potentially be used in isolation to estimate low-level tornado intensity. The proposed estimation is by way of a linear regression model, and application of this model is relevant only once a tornado is already confirmed.

1. Introduction

Visual observations of tornadoes and/or the existence of tornado damage currently provides the sole evidence of tornadogenesis in association with a mesocyclone or other radar-detected storm-scale vortex. The severity of the tornado damage, as expressed in terms of the Fujita (F)—and now enhanced Fujita (EF)—scales (Fujita 1971; McDonald and Mehta 2006), is currently the only means of estimating the intensity of tornadoes, radar detected or otherwise.

The limitations of the damage-based record of tornado occurrence and intensity are well known (e.g., Doswell et al. 2009; see also Diffenbaugh et al. 2008). We are particularly motivated by the latter and herein take the first step toward developing an alternative means of intensity estimation.

Relevant previous studies have focused mostly on relationships either 1) between Weather Surveillance Radar-1988 Doppler (WSR-88D; see Crum and Alberty 1993) measurements and damage (Burgess et al. 2002) or 2) between mobile radar measurements and damage (Wurman and Alexander 2005) or visual characteristics (Atkins et al. 2012). As described in sections 2 and 3, our focus is on WSR-88D measurements of the translating tornadic flow as compared with (semi-) coordinated measurements obtained near the surface with mobile radar. This approach is tangential to additional work by Burgess et al. (2002), although they did not include the effects of translation and considered only one event.

From a small yet fairly broad sample of tornadoes, we will show in section 3 evidence of a high linear correlation between WSR-88D and corresponding mobile-radar measurements of tornadoes. Of course, Doppler-radar sampling of atmospheric vortices is not without issues, and we attempt to address some of them in section 4. A discussion of other limitations is provided in section 5, followed by some concluding remarks in section 6.

Corresponding author address: Mallie Toth, Dept. of Earth, Atmospheric, and Planetary Sciences, Purdue University, 550 Stadium Mall Dr., West Lafayette, IN 47907.
E-mail: toth2@purdue.edu

DOI: 10.1175/WAF-D-12-00019.1

TABLE 1. List of events included in the statistical model, ranges of the events to both the DOW and WSR-88D, model-derived maximum wind speed M from Eq. (6), and comparison of overall (E)F-scale ratings from the National Climatic Data Center's *Storm Data* publication from 1995 to 2011 with those derived by the statistical model. An asterisk indicates a reported multiple-vortex event. Boldface rows indicate the 14 events (minus the two excluded 2007 events) that met the criteria that are described in section 2.

Date	Location	DOW time (UTC)	DOW ΔV (m s^{-1})	Height (°)	WSR-88D time (UTC)	WSR-88D ΔV (m s^{-1})	DOW range (km)	WSR-88D range (km)	*Storm Data* F/EF scale	M (m s^{-1})	Model-based F scale	Model-based EF scale
16 May 1995	**Hanston, KS**	**0147:18**	**82.6**	**0**	**0147:40**	**65**	**13**	**52**	**3**	**62.88**	**2**	**3**
2 Jun 1995	Dimmitt, TX	0105:35	139.2	1	0112:38	54.1	3	109	2	52.10	2	2
25 May 1996	**Friona, TX**	**2235:46**	**114.2**	**0**	**2248:50**	**64**	**12**	**90**	**0**	**64.38**	**2**	**3**
31 May 1996	Rolla, KS	2300:27	82.6	2.1	2257:22	57	3	170	0	55.00	2	2
10 Apr 1997	**Tulia, TX**	**2224:50**	**54.1**	**3.2**	**2235:37**	**46.5**	**6**	**81**	**0**	**53.64**	**2**	**2**
26 May 1997	**Kiefer, OK**	**2239:00**	**90.2**	**3.4**	**2231:54**	**48.6**	**8**	**53**	**1**	**37.69**	**1**	**1**
30 May 1998	**Spencer, SD***	**0134:28**	**205.5**	**1.4**	**0129:15**	**111.9**	**2**	**75**	**5**	**98.70**	**4**	**5**
1 May 1999	**Tarzan, TX**	**2240:11**	**65.8**	**2**	**2243:18**	**42.5**	**2**	**44**	**0**	**38.97**	**1**	**1**
3 May 1999	**Moore, OK***	**0021:59**	**177**	**0.2**	**0037:31**	**92.9**	**3.5**	**17**	**5**	**83.46**	**3**	**4**
31 May 1999	**Sitka, KS**	**2327:59**	**65**	**1.9**	**2321:06**	**48**	**16**	**66**	**1**	**57.88**	**2**	**2**
3 Jun 1999	Almena, KS*	0042:33	140.8	0	0026:36	54.6	4	120	3	52.60	1	2
4 Jun 1999	**Thedford, NE**	**0243:56**	**96.4**	**1**	**0229:06**	**74.8**	**10**	**21**	**2**	**84.30**	**3**	**4**
5 Jun 1999	Bassett, NE	0117:43	77.4	1	0122:19	54.3	3	108	1	52.30	2	2
17 May 2000	Brady, NE	2225:17	126.1	0.3	2222:54	55.3	24	112	3	53.30	2	2
26 May 2000	Throckmorton,TX	0020:43	39.7	3	0005:32	35	7	197	0	33.00	1	0
06 May 2001	Marietta, OK	2207:42	52.8	1.3	2214:54	41.5	9	139	0	39.50	1	1
24 May 2004	**Hebron, NE***	**2121:10**	**80.5**	**4.8**	**2111:06**	**62.6**	**12**	**62**	**1**	**59.44**	**2**	**2**
13 May 2005	Seymour, TX	0030:50	151.3	1	0025:41	72.9	6	116	3	70.90	3	3
9 Jun 2005	Hill City, KS	2220:59	96.3	1.4	2219:07	91.5	2	150	0/1	89.50	3	5
15 Jun 2005	Trego Center, KS	0053:19	107.6	2.4	0043:32	81.5	8	115	0	79.50	3	4
21 Apr 2007	TX Panhandle	0202:23	113.1	1	0210:37	67	7	45	1	43.50	1	1
23 Apr 2007	Protection, KS	0132:20	81.9	0.3	0124:41	54	7	75	0	37.00	1	0
10 May 2008	**Stuttgart, AR**	**0112:42**	**113.4**	**2**	**0105:57**	**81**	**3**	**82**	**3**	**91.25**	**3**	**5**
5 Jun 2009	**Goshen County, WY**	**2216:50**	**108.6**	**0.4**	**2202:00**	**53**	**5**	**64**	**2**	**52.67**	**2**	**2**

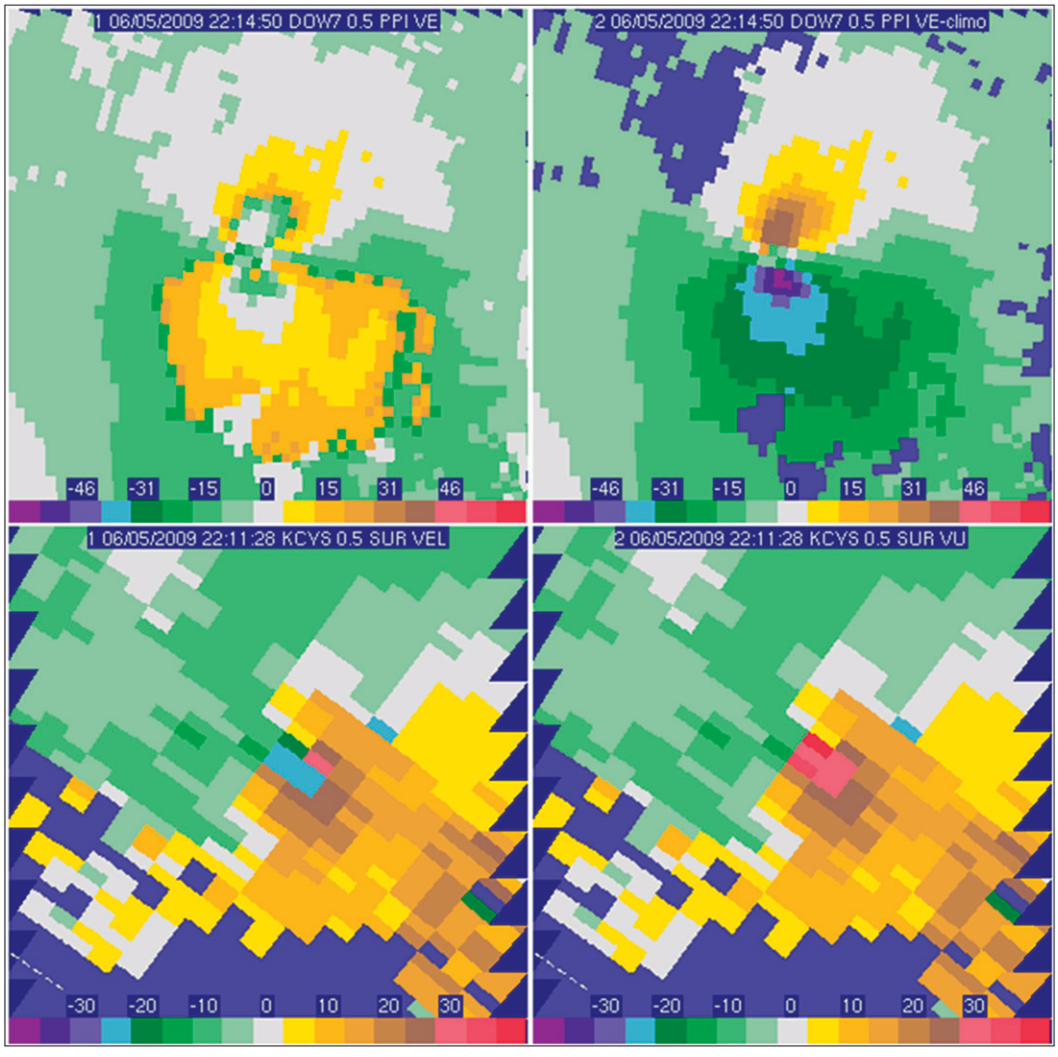

FIG. 1. Comparison of (left) raw and (right) quality-controlled (top) DOW and (bottom) WSR-88D data.

2. Data and methods

In this study we make use of plan position indicator (PPI) data collected by the Doppler on Wheels radar (DOW). The DOW is a mobile, 3-cm-wavelength, ~1°-beamwidth radar designed to sample hazardous or short-lived phenomena on fine temporal and spatial scales (Wurman et al. 1997). Because of its mobility and scanning capabilities, the DOW is able to sample the tornado much closer to ground level, in more frequent update intervals, and at higher resolution than is the WSR-88D. Available in situ data show little reduction in the wind speeds between low-level DOW observations and 3-m in situ wind measurements (Wurman et al. 2007, 2013). Limitations of DOW data have been discussed in detail by Wurman et al. (2007).

As alluded to in section 1, we also make use of corresponding PPI data collected at 0.5° elevation by the nationwide network of WSR-88Ds. The WSR-88Ds operate at 10-cm wavelength and have half-power beamwidths of ~1°. Scans by the WSR-88Ds cover most of the area of the continental United States, although in much of this area the beams are well above the ground, even at the lowest elevation angles. Furthermore, the width of the radar beam is often too large to effectively sample the tornadic circulation (Alexander and Wurman 2004). Thus, the WSR-88Ds often do not provide velocity estimates of the tornado itself but rather of its parent mesocyclone (Stumpf et al. 1998) and/or its tornadic vortex signature, which is a coarse representation of the tornado (Mitchell et al. 1998).

We selected tornado cases on the basis of the existence of proximal WSR-88D data during the interval of

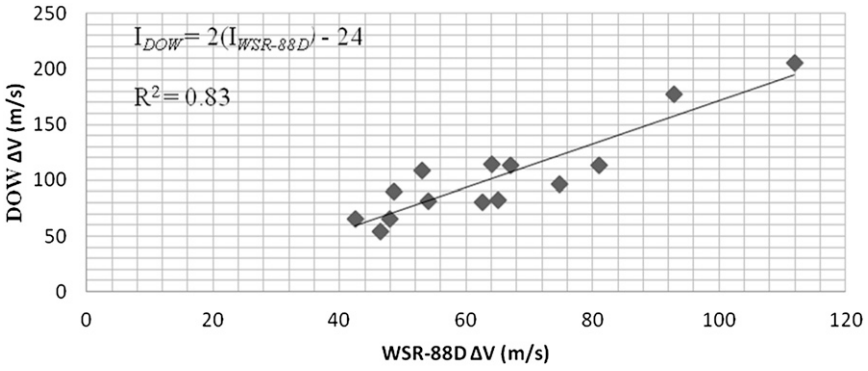

FIG. 2. Scatterplot showing the maximum differential velocities, and hence intensity *I*, observed by the DOW and WSR-88D for the 14 tornadic events that occurred within 100 km of a WSR-88D.

DOW scans. The WSR-88D velocity data in particular were required to exhibit an unambiguous mesocyclone or tornadic-vortex signature; severe velocity aliasing [as in the event described by Wakimoto et al. (2004)] or distant radar ranges constituted two reasons why cases failed to meet this requirement and therefore were excluded from our dataset. As justified in section 4, we imposed an additional constraint that the proximal WSR-88D be within 100 km of the tornado. The respective WSR-88D and DOW data archives produced 14 events that met these criteria (see Table 1). Although this is admittedly a relatively small dataset, it does offer a wide range of damage ratings and tornado sampling from a wide range of DOW and WSR-88D distances.

In the interest of restricting the DOW data to the lower levels of the tornadic circulation, only PPI data collected below 5° elevation and within 20 km of the DOW were considered. In the optimum case, we would have preferred to limit the DOW data analysis to the lowest scan in a volume or a specific height, but it was not feasible to do so because of issues such as beam blockage as well as varied scanning strategies.

Both DOW and WSR-88D data were edited using the National Center for Atmospheric Research ''Soloii'' software (Oye et al. 1995). For DOW data in particular, thresholds of 0.25–0.30 were applied in the normalized coherent power field to minimize contaminated data, and regions of high reflectivity and near-zero velocity values were also used to identify and remove ground clutter; Alexander and Wurman (2004) provide additional information on the quality-control procedures applied to these data. In the event of velocity aliasing, a common occurrence in data from both radars, the velocity data were manually unfolded. An example of DOW and WSR-88D data prior to and after the quality-control procedure is shown in Fig. 1.

The WSR-88D and DOW velocities in scans of tornadoes/parent vortices were related through linear regression of differential velocity ΔV:

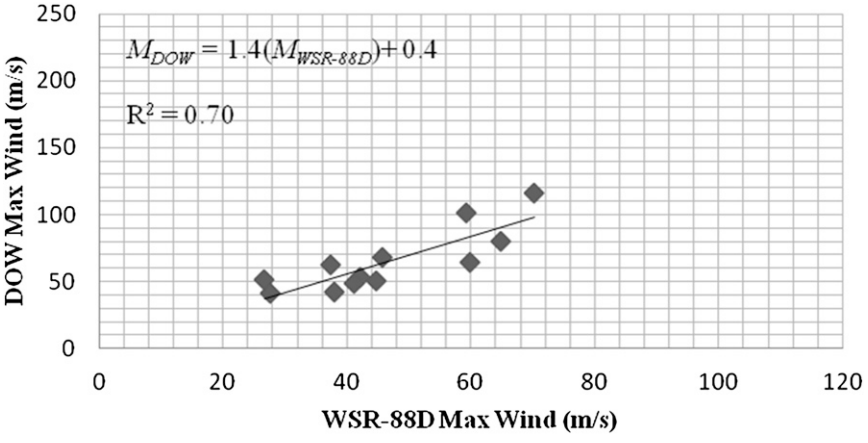

FIG. 3. Scatterplot comparing the average DOW and WSR-88D translational speed for 12 of the 14 events within 100 km of the WSR-88D.

TABLE 2. The Joplin and Sawyerville events from 2011, with maximum model-derived wind speeds determined using Eq. (6).

Date	Location	Time (UTC)	WSR-88D ΔV (m s^{-1})	WSR-88D range (km)	*Storm Data* EF scale	M (m s^{-1})	Model-derived EF scale
22 May 2011	Joplin, MO	2244:08	102.2	99	5	91.09	5
27 Apr 2011	Sawyerville, AL	2314:18	83.4	76	3	90.60	5

$$\Delta V = V_{\max} - V_{\min}, \tag{1}$$

where $V_{\max}$ ($V_{\min}$) is the maximum (minimum) ground-relative radial velocity across the tornado or mesocyclone. The use of ΔV provided us with a simple quantification of vortex intensity; ΔV is also a commonly diagnosed quantity in automated algorithms (e.g., Stumpf et al. 1998; Mitchell et al. 1998). For each case, the maximum ΔV from the DOW data was determined and then equated to I_{DOW}, our parameter representing the near-ground-level intensity of the tornado. The WSR-88D 0.5° data were then analyzed over the 15 min (~three volume scans) prior to and following the I_{DOW} time to determine the associated WSR-88D maximum ΔV ($I_{\text{WSR-88D}}$). Note that this time window accounted for the differing scanning strategies employed by the two radars; it also allowed for collection of multiple samples of the vortex by the WSR-88D, in different radar-beam-relative locations owing to tornado movement and evolution between radar scans (see section 4). These values then formed the basis of our statistical model:

$$I_{\text{DOW}} = \alpha(I_{\text{WSR-88D}}) + \beta, \tag{2}$$

where α and β are the empirically determined linear regression coefficients.

Because both translation and rotation contribute to the tornadic winds, we also examined the translational speed of the storm and its associated tornado. The translational speed T of each vortex[1] as measured by both radars was approximated using the distance traveled between successive scans (i.e., times) and then was averaged over a 15–30-min period. This was used to determine a relationship between the two independent estimates of maximum wind speed M:

$$M_{\text{DOW}} = \lambda(M_{\text{WSR-88D}}) + \mu, \tag{3}$$

where λ and μ are empirically determined linear regression coefficients and

$$M = I/2 + T. \tag{4}$$

Note that the use of $I/2$ in Eq. (4) follows from Eq. (1) and contributes an estimate of the tangential component of velocity.

3. Results

We begin with vortex intensity I. Our derived statistical relationship between the WSR-88D and DOW quantifications of 14 tornadic events was

$$I_{\text{DOW}} = 2.0(I_{\text{WSR-88D}}) - 24, \tag{5}$$

with a linear correlation coefficient squared of $R^2 = 0.83$ and statistical significance of the slope at the 95% confidence interval, determined using a t test (Fig. 2). We therefore conclude that the DOW and WSR-88D intensity quantifications are highly correlated, albeit with a caveat that this conclusion is based on a relatively small sample. On this note, we reiterate that the events in our sample had (E)F ratings ranging from F0 to F5 and were located at various distances to both the DOW and WSR-88D, suggesting potential broad applicability of the statistical model.

As previously mentioned, both translation and rotation of the tornado contribute to the total tornadic winds. Using Eq. (4) to account for a mean translation in each of our events, we determined the following statistical relationship:

$$M_{\text{DOW}} = 1.4M_{\text{WSR-88D}} + 0.4, \tag{6}$$

which has a linear correlation coefficient squared of $R^2 = 0.7$ (Fig. 3). Hence, again on the basis of a relatively small sample, we can also conclude that the maximum wind speeds from the DOW and WSR-88D are highly correlated.

The suggested application of a statistical model like Eq. (6) is to use it for estimation of maximum tornadic wind speeds from WSR-88D measurements; this approach thus avoids the issues of damage assessments alluded to in section 1. A frequent question raised about Eq. (6), however, is how well its estimates would agree with damage-based estimates. Although doing so is a bit circular in logic, we applied Eq. (6) to each of our events using $M_{\text{WSR-88D}}$ and then converted the resultant

[1] Because of georeferencing errors in the DOW data, the two events from 2007 were not included in this portion of the analysis.

TABLE 3. Joplin and Sawyerville events from 22 May 2011 and 27 Apr 2011, respectively. Damage-survey EF-scale values given at each point correspond approximately to the WSR-88D location at each point (National Oceanic and Atmospheric Administation 2011a,b).

M (m s^{-1})	Model-derived EF	WSR-88D-based lat, lon (°)	Damage-survey EF	Damage-survey lat, lon (°)
		Joplin		
91.09	5	37.0672, −94.4997	5	37.0642, −94.5071
87.24	4	37.0646, −94.4661	5	37.0684, −94.4778
72.12	3	37.0556, −94.4232	3	37.0648, −94.4465
88.64	4	37.0365, −94.3745	0	37.0383, −94.3730
		Sawyerville		
82.55	4	32.7987, −87.6690	3	32.8030, −87.6552
86.05	4	32.8331, −87.6233	3	32.8196, −87.6349
82.90	4	32.8563, −87.5662	3	32.8769, −87.5234
90.60	5	32.8839, −87.5140	3	32.8769, −87.5234
76.95	4	32.9079, −87.4507	2	32.9047, −87.4420
72.75	3	32.9816, −87.2605	3	32.9880, −87.2426

model-estimated winds to (E)F-scale rankings. As shown in Table 1, the model-derived rankings are generally within a category of the *Storm Data* rankings, with a few exceptions. Although we cannot rule out intrinsic error in the radar measurements and statistical model, some of these differences are simply the result of a comparison between the value range inherent in (E)F-scale categories and the single value from the model (see Table 1). Another contributor to the differences is the fidelity or representativeness of the tornado damage relative to the true tornado intensity. It is possible for the damage to lead to under- or overestimates of intensity (e.g., Wurman and Alexander 2005). Indeed, this situation is a primary motivation for the proposed approach.

Further evaluation is afforded by application of Eq. (6) to events that are not in our training dataset. The independent samples include two recent events that were well surveyed and documented: the 22 May 2011 Joplin, Missouri, tornado and the 27 April 2011 Sawyerville, Alabama, tornado (Table 2). The model-estimated wind speeds from the two 2011 events agree well with damage-survey estimates at specific locations along the paths of the tornadoes (Table 3). A notable exception is the final point on the Joplin event, in which the model yields an equivalent EF5 rating at a location where EF0 damage was denoted. At this location, high-resolution aerial imagery was utilized to establish the lack of tree damage; it is plausible that the tornado may have dissipated briefly at this point, and the regression would no longer be valid without the presence of a tornado (National Oceanic and Atmospheric Administation 2011a).

4. Evaluation of radar sampling

The regression model is limited by the independent variable(s), here the WSR-88D estimate of the parent vortex, which in turn in is inherently limited by increases in beam height and thus height of vortex sampling with increasing range, beam broadening with increasing range, and the chance positioning of a vortex relative to the center of the radar beam (e.g., Wood and Brown 1997). To quantify the potential effects of the latter two limitations on our linear regression, we used the radar simulator of Wood and Brown (1997). The simulator is two dimensional and assumes a uniform radar reflectivity field and a Rankine-combined vortex.

Our prescribed parent vortex (mesocyclone) has a 2.5-km radius of maximum winds and maximum radial velocities of ±25 m s^{-1}; in the context of our regression variable, the true vortex has a differential velocity of 50 m s^{-1}. This vortex was then sampled by the Wood–Brown radar simulator at various ranges (50–200 km)

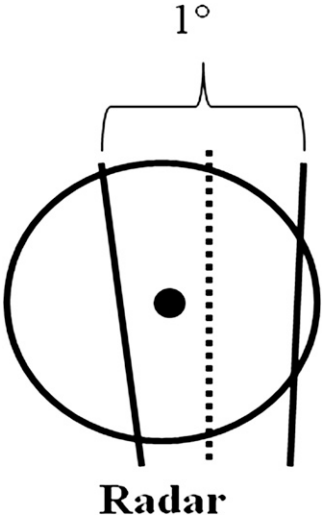

FIG. 4. An example of an azimuthally offset radar beam relative to the vortex center. The black dot represents the true center of the vortex, and the dotted line represents the center of our modeled 1° radar beam. The azimuthal difference between the vortex center dot and radar beam centerline represents our azimuthal offset.

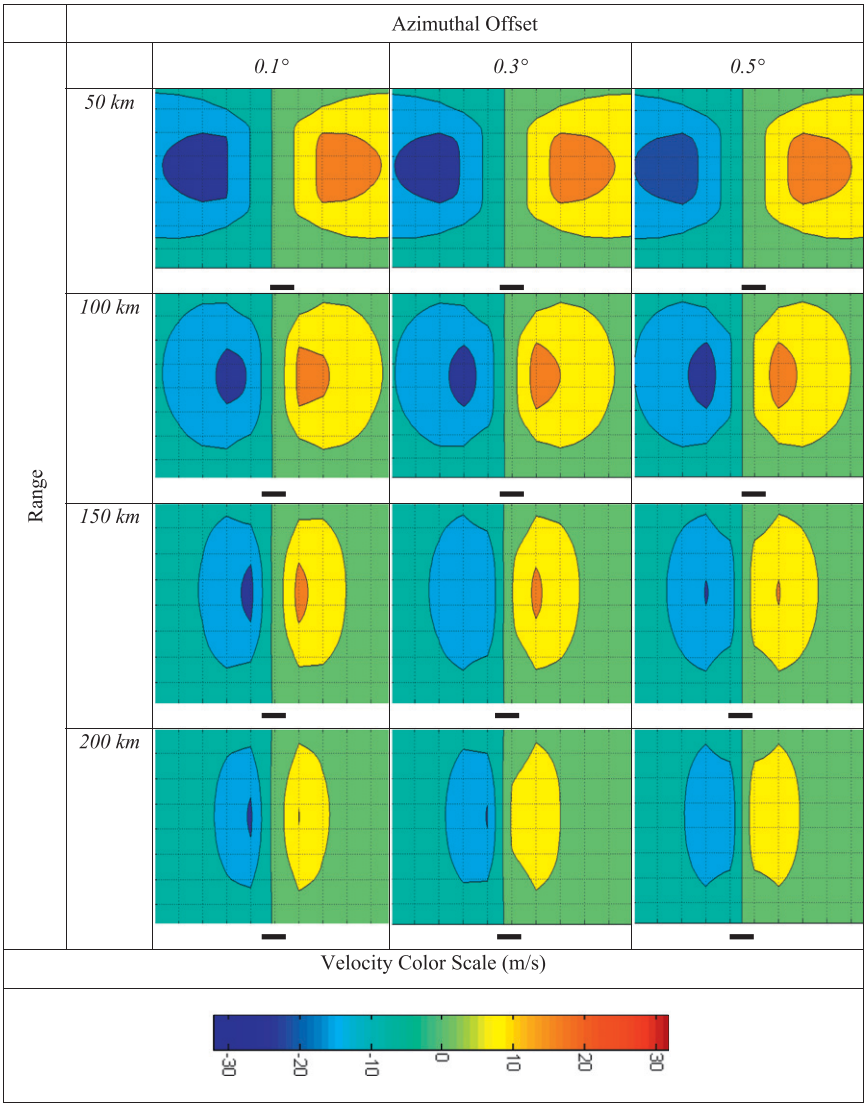

FIG. 5. Output from the radar model of an idealized Rankine-combined vortex with maximum radial velocities of ±25 m s^{-1}. Grids are marked at 1° in the x direction and 1 km in the y direction; the black bar in each panel represents the approximate size of a 1° × 250 m radar bin. The idealized vortices have been sampled by the model at various ranges and azimuthal offsets from the radar.

and azimuthal offsets (0.0°–0.5°, where 0.5° is the maximum offset for the 1° beam used here; see also Fig. 4). As depicted in Fig. 5, the maximum radial velocities (and ΔV) in the radar-sampled vortex generally decrease with increasing range and azimuthal offset (Table 4, top rows). Notice that a perfectly centered vortex relative to the radar beam at 50-km range from the radar would experience less than 1 m s^{-1} degradation in the radar-sampled differential velocity. A vortex with an offset of 0.5° at 200 km from the radar, however, would be perceived as ~23 m s^{-1} weaker than its true intensity; a vortex with an offset of 0.5° at 100 km from the radar would be perceived as ~9 m s^{-1} weaker than its true intensity. Prescribed vortices with 1.25- and 5-km radii of maximum winds exhibit a similar decrease in sampled intensity with range (Table 4, middle and bottom rows). The effect of offset depends on the core radius (e.g., see Fig. 4), with the 1.25-km vortex more favorably sampled in intensity with larger offset (Table 4).

These experiments bear out the well-behaved decrease in radar-sampled vortex intensity with range; we address this limitation in the regression model with a restriction to tornado events with ranges of less than 100 km. The less-well-behaved change in sampled intensity with azimuthal offset merits further consideration, because it suggests a sensitivity of the regression model results to a chance

TABLE 4. Maximum differential velocity (m s^{-1}) perceived by the radar model at various ranges and azimuthal offsets of the idealized vortices for three different radii of maximum winds.

	Azimuthal offset			
Range	0.0°	0.1°	0.3°	0.5°
2500-m radius				
50 km	49.20	44.78	43.71	42.48
100 km	36.36	36.82	39.74	40.80
150 km	36.88	36.49	33.59	32.76
200 km	33.42	33.12	30.75	27.06
1250-m radius				
50 km	36.27	36.76	39.67	40.73
100 km	33.37	33.07	30.71	27.03
150 km	25.45	25.34	24.33	26.13
200 km	20.08	20.06	20.66	23.16
5000-m radius				
50 km	47.01	46.95	46.61	46.89
100 km	44.98	44.84	43.76	42.50
150 km	42.92	42.71	41.11	38.63
200 km	36.41	36.85	39.77	40.84

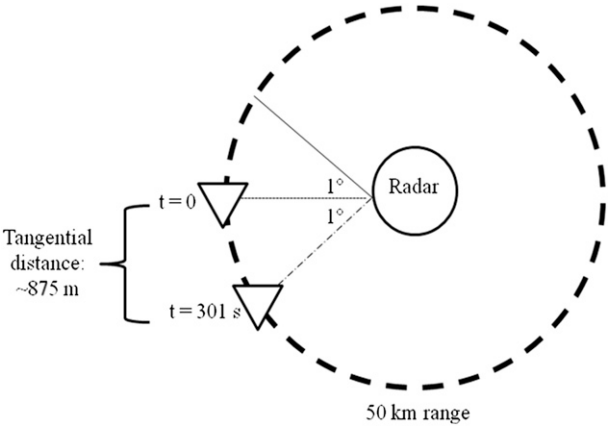

FIG. 6. A vortex traveling along different radials at 50-km range from the radar will be first sampled at some time $t = 0$ at a specific azimuthal offset in the radar beam. One volume scan and one additional beam later, if one ignores the arc of the radial in favor of simple right-triangle geometry, the vortex would have had to maintain a translational speed of ~3 m s^{-1} to be sampled at the exact same offset again.

positioning of a vortex relative to the beam center. In this regard, it is relevant to ask how often the parent vortex would be radar sampled in a worst-case azimuthal offset for the entire lifetime of the tornado. Imagine a tornado and parent vortex that at time $t = 0$ are located and sampled in a beam 50 km from the radar. Let the vortex move such that it maintains a constant 50-km range from the radar (see Fig. 6). After 300 s (a typical volume-scan period), assume that the vortex has moved into and is sampled by the beam adjacent to the initial beam; that is, it has moved ~875 m (the linear width of a 1° beam at 50 km) in 300 s. For the vortex to have been sampled at the exact same azimuthal offset after one radar scan, it must have moved at a specific speed, in this case, 3 m s^{-1}. The implication here is that the vortex must maintain this specific and constant speed (or some multiple thereof) for it to be sampled at the same azimuthal offset over the entire period of consideration (30 min in the current study). This same conclusion is reached for hypothetical vortices moving along radials at other radar ranges.

Of course, real tornadoes tend not to maintain such a constant translational speed and also tend not to move at constant range. Thus, it seems reasonable to assume that the tornado would not be sampled in a worst-case offset at all times; in particular, this means that for at least some times during the 30-min intervals of our WSR-88D data consideration it is reasonable to assume that the vortex would be sampled at various azimuthal offsets, perhaps including the best possible offset.

5. Discussion

At a fundamental level, one should expect a relationship between the intensity of the tornado and the intensity of the parent circulation. This follows from theoretical arguments that are based on conservation of angular momentum and also in terms of solutions to simplified versions of the vertical vorticity equation, for example, $\zeta(t) = \zeta_0 \exp(\delta t)$, where ζ_0 is some initial vertical vorticity that is subject to vortex stretching over time t and δ is an assumed mean convergence. Simply put, the larger the ambient vertical vorticity or circulation is, the larger is the vorticity or circulation upon contraction into a tornado.

The results from section 4 are useful in illustrating possible radar-sampling effects on vortex detection and quantification. Nonetheless, the information that can be garnered from this radar simulator is limited by assumptions of a Rankine-combined vortex and lack of variation of the tornado with height. Complications may also arise in estimating the ground-level impacts of multiple-vortex tornadoes, which often exhibit relatively more temporal and spatial variations in structure and vortex strength (see Wurman 2002).

6. Conclusions and future work

Our results show high linear correlation between WSR-88D velocity estimates of parent tornadic vortices and near-ground tornadic wind speeds as observed by mobile radar (the DOW). The suggestion from this work is that the WSR-88D can potentially be used in isolation to estimate low-level tornado intensity; this possibility is supported by the independent work of Thompson et al. (2012), and ongoing research at the Warning Decision Training Branch of the National Weather Service

(J. LaDue 2011, personal communication). The proposed estimation is by way of a linear regression model, and application of this model is relevant only *once a tornado is already confirmed*. The particular model presented herein is based on a dataset of tornadic events that range in intensity and radar distance, but this dataset is relatively small. More events will be incorporated into the statistical analysis as they become available so as to provide a more robust relationship.

Experiments with a radar simulator demonstrated that the radar-sampling effects on vortex detection and quantification should not invalidate the proposed method, provided that radar range restrictions are made and that sufficient time is allowed for the tornado/parent vortex to reposition itself relative to the radar beam. An uncertainty not addressed here is that of the radar sampling of sub-tornado-scale vortices. Hence, future work will investigate multiple-vortex radar sampling considerations using three-dimensional numerical simulations of tornadic vortices. Additional future work will also consider higher-resolution WSR-88D data.

Acknowledgments. The first author received partial support from National Science Foundation (NSF) Grant ATM-0758588. The authors acknowledge the NSF for its support of the Second Verification of the Origins of Rotation in Tornadoes Experiment (VORTEX2) project, as well as of deployments of the DOW, which is a Lower Atmospheric Observing Facility. The authors also thank all participants of the VORTEX(1-2) and Radar Observations of Tornadoes and Thunderstorms Experiment (ROTATE) field projects and the personnel of the Center for Severe Weather Research. This research represents a contribution to the Clouds, Climate, and Extreme Weather initiative at Purdue University.

REFERENCES

Alexander, C. R., and J. Wurman, 2004: Comparison between DOW observed tornadoes and parent mesocyclones observed by WSR-88Ds. Preprints, *22nd Conf. on Severe Local Storms,* Hyannis, MA, Amer. Meteor. Soc., 13.4. [Available online at https://ams.confex.com/ams/11aram22sls/webprogram/Paper81767.html.]

Atkins, N. T., A. McGee, R. Ducharme, R. M. Wakimoto, and J. Wurman, 2012: The LaGrange tornado during VORTEX 2. Part II: Photogrammetric analysis of the tornado combined with dual-Doppler radar data. *Mon. Wea. Rev.,* **140,** 2939–2958.

Burgess, D. W., M. A. Magsig, J. Wurman, D. C. Dowell, and Y. Richardson, 2002: Radar observations of the 3 May 1999 Oklahoma City tornado. *Wea. Forecasting,* **17,** 456–471.

Crum, T. D., and R. L. Alberty, 1993: The WSR-88D and the WSR-88D Operational Support Facility. *Bull. Amer. Meteor. Soc.,* **74,** 1669–1687.

Diffenbaugh, N. S., R. J. Trapp, and H. E. Brooks, 2008: Challenges in identifying influences of global warming on tornado activity. *Eos, Trans. Amer. Geophys. Union,* **89,** 553–554.

Doswell, C. A., III, H. E. Brooks, and N. Dotzek, 2009: On the implementation of the enhanced Fujita scale in the USA. *Atmos. Res.,* **93,** 554–563.

Fujita, T. T., 1971: Proposed characterization of tornadoes and hurricanes by area and intensity. University of Chicago Satellite and Mesometeorology Research Project Research Paper 91, 42 pp.

McDonald, J. R., and K. C. Mehta, 2006: A recommendation for an enhanced Fujita scale (EF-scale), revision 2. Texas Tech University Wind Science and Engineering Research Center Rep., 110 pp. [Available online at http://www.depts.ttu.edu/weweb/Pubs/fscale/EFScale.pdf.]

Mitchell, E. D., S. V. Vasiloff, G. J. Stumpf, A. Witt, M. D. Eilts, J. T. Johnson, and K. W. Thomas, 1998: The National Severe Storms Laboratory tornado detection algorithm. *Wea. Forecasting,* **13,** 352–366.

National Oceanic and Atmospheric Administration, cited 2011a: Joplin tornado survey. Springfield, MO, National Weather Service Forecast Office. [Available online at http://www.crh.noaa.gov/sgf/?n=event_2011may22_survey#Joplin.]

——, cited 2011b: Sawyerville-Eoline (Greene, Hale and Bibb Counties) EF-3 tornado, April 27, 2011. Birmingham, AL, National Weather Service Forecast Office. [Available online at http://www.srh.noaa.gov/bmx/?n=event_04272011sawyerville.]

Oye, R., C. Mueller, and S. Smith, 1995: Software for radar data translation, visualization, editing, and interpolation. Preprints, *27th Conf. on Radar Meteorology,* Vail, CO, Amer. Meteor. Soc., 359–361.

Stumpf, G. J., A. Witt, E. D. Mitchell, P. L. Spencer, J. T. Johnson, M. D. Eilts, K. W. Thomas, and D. W. Burgess, 1998: The National Severe Storms Laboratory mesocyclone detection algorithm for the WSR-88D. *Wea. Forecasting,* **13,** 304–326.

Thompson, R. L., B. T. Smith, J. S. Grams, A. R. Dean, and C. Broyles, 2012: Convective modes for significant severe thunderstorms in the contiguous United States. Part II: Supercell and QLCS tornado environments. *Wea. Forecasting,* **27,** 1136–1154.

Wakimoto, R. M., H. Cai, and H. V. Murphey, 2004: The Superior, Nebraska, supercell during BAMEX. *Bull. Amer. Meteor. Soc.,* **85,** 1095–1106.

Wood, V. T., and R. A. Brown, 1997: Effects of radar sampling on single-Doppler velocity signatures of mesocyclones and tornadoes. *Wea. Forecasting,* **12,** 928–938.

Wurman, J., 2002: The multiple-vortex structure of a tornado. *Wea. Forecasting,* **17,** 473–505.

——, and C. R. Alexander, 2005: The 30 May 1998 Spencer, South Dakota, storm. Part II: Comparison of observed damage and radar-derived winds in the tornadoes. *Mon. Wea. Rev.,* **133,** 97–119.

——, J. Straka, E. Rasmussen, M. Randall, and A. Zahrai, 1997: Design and deployment of a portable, pencil-beam, pulsed, 3-cm Doppler radar. *J. Atmos. Oceanic Technol.,* **14,** 1502–1512.

——, C. Alexander, P. Robinson, and Y. Richardson, 2007: Low-level winds in tornadoes and potential catastrophic tornado impacts in urban areas. *Bull. Amer. Meteor. Soc.,* **88,** 31–46.

——, K. Kosiba, and P. Robinson, 2013: In situ, Doppler radar, and video observations of the interior structure of a tornado and wind-damage relationship. *Bull. Amer. Meteor. Soc.,* in press.